ELSEVIER

Polymer 40 (1999) 6225–6234

polymer

Precipitation polymerization of acrylic acid in toluene. II: mechanism and kinetic modeling

Charun Bunyakan[a], Luc Armanet[b], David Hunkeler[b,*]

[a]*Department of Chemical Engineering, Vanderbilt University, Nashville, TN 37235, USA*
[b]*Laboratory of Polymers and Biomaterials, Swiss Federal Institute of Technology, CH-1015 Lausanne, Switzerland*

Received 19 March 1998; received in revised form 10 August 1998; accepted 19 November 1998

Abstract

Although the kinetics of the precipitation polymerization of acrylic acid were investigated by a number of researchers, no mechanism has been proposed which considers the reaction in both continuous and dispersed phases. In this article a general mechanism is developed for the precipitation polymerization of acrylic acid in toluene. It is compared with experimental data and is found to predict rate of polymerization and molecular weight reasonably well. The mechanism consists of the initiation, propagation, transfer and termination reaction, which are common to all free-radical polymerizations. It also found that monomer-enhanced decomposition and transfer to monomer are the dominant mechanism for initiation and chain termination, respectively. The kinetic parameters were evaluated against experimental data.

Keywords: Acrylic acid; Polyacrylic acid; Polymer reaction engineering

1. Introduction

An understanding of the mechanism and kinetics of the precipitation polymerization process is essential for the optimization and control of commercial polyacrylic acid production. The molecular weight of the polymer, the rate of polymerization, and the conversion are influenced strongly by the elementary reaction scheme. Although free-radical polymerizations of acrylic acid were investigated by a number of researchers, as discussed in Ref. [1], relatively little effort has been dedicated to the precipitation polymerization of acrylic acid in the open literature.

The mechanism and kinetic model for the precipitation polymerizations are more complicated than for solution processes because of a physical transformation from an initially homogeneous system to a heterogeneous mixture during the course of reaction. An extensive investigation of the precipitation polymerization of acrylic acid, chemically initiated with 2,2′-azobis (2,4-dimethyl valeronitrile), was also carried out by Avela, et al. [2,3]. A kinetic model for precipitation polymerization of acrylic acid in toluene was also developed by Reichert and coworkers, which neglected monomer consumption in the homogeneous phase and considered the heterogeneous polymer phase to be the only locus of polymerization. This article reports an attempt to investigate the synthetic mechanism of the precipitation polymerization of acrylic acid in toluene with the aim of developing a general mechanistic model, which considers the polymerization reactions in both the continuous and dispersed phases. This model will be shown to be able to predict the rate of precipitation polymerization and the molecular weight of polymer as a function of reaction conditions.

2. Experimental

Acrylic acid was isothermally polymerized via a precipitation polymerization in toluene at various monomer and initiator concentrations over the temperature ranges of 40°C–50°C. The experimental procedures, and results, are detailed in Ref. [1].

Simulations based on the kinetic model, developed in the following section, were carried out by numerically solving ordinary differential equations using a method based on a 6th order Runge–Kutta technique.

3. Results and discussion

The following mechanism has been developed based on

* Corresponding author. Tel.: + 41-021-693-3114; fax: + 41-021-693-5690.

E-mail address: david.hunkeler@epfl.ch (D. Hunkeler)

0032-3861/99/$ - see front matter
PII: S0032-3861(98)00837-4

literature studies of the solution polymerization of acrylic acid [4–7], precipitation polymerization [2,3], heterophase polymerization in general [8], by analogy to the polymerization mechanism found from other water soluble monomers such as acrylamide [9], and the observation from the experiments in Ref. [1]. The mechanism can be divided into a series of reactions in the continuous and dispersed phase as well as some mass transfer and partitioning steps.

3.1. Mechanism

3.1.1. Reactions in the continuous phase (solvent, monomer and initiator):

1. Initiator decomposition:

$$I_c \xrightarrow{k_{dc}} 2R^{\bullet}_{in,c} \quad (1)$$

Where I and $R^{\bullet}_{in}$ are the symbols for initiator and primary radicals respectively. The subscript "c" designates a continuous phase species. As was discussed in an earlier article [1] this chemical decomposition step is negligible compared with the monomer-enhanced decomposition.

2. Monomer-enhanced decomposition of initiator [5]:

$$I_c + M_c \xrightarrow{k'_{dc}} R^{\bullet}_{1,c} + R^{\bullet}_{in,c} \quad (2)$$

3. Initiation:

$$R^{\bullet}_{in,c} + M_c \xrightarrow{k_{p1c}} R^{\bullet}_{1,c} \quad (3)$$

4. Propagation:

$$R^{\bullet}_{r,c} + M_c \xrightarrow{k_{pc}} R^{\bullet}_{r+1,c} \quad (4)$$

5. Transfer [5,7]:

$$R^{\bullet}_{r,c} + M_c \xrightarrow{k_{fmc}} M^{\bullet}_c + P_r \quad (5)$$

6. Transfer:

$$R^{\bullet}_{r,c} + S_c \xrightarrow{k_{fsc}} S^{\bullet}_c + P_r \quad (6)$$

7. Termination [7]:

$$R^{\bullet}_{r,c} + R^{\bullet}_{s,c} \xrightarrow{k_{tdc}} P_r + P_s \quad (7)$$

where $M, M^{\bullet}$, $R^{\bullet}_1$, $R^{\bullet}_r, S$, $S^{\bullet}$, P_r, P_s are the symbols for monomer, monomeric radicals, a macroradical of length 1, macroradical containing r monomer units, solvent, solvent radicals, dead polymer containing r repeating units, and dead polymer containing s repeat units, respectively. Step 2 of this scheme was originally postulated by Manickam [5] for aqueous solution and was found to be valid in the precipitation polymerization in toluene based on an approximately sesquimolecular (1.5 order) rate dependence on monomer [1]. Both acrylic acid (5) and toluene (6) are known to have labile hydrogen groups and participate in transfer reactions, though the rate of transfer to solvent (toluene) is much smaller than to monomer (acrylic acid).

3.1.2. Mass transfer between continuous and dispersed phases

8. Initiator:

$$I_c \xleftrightarrow{\varphi_I} I_d$$

9. Monomer:

$$M_c \xleftrightarrow{\varphi_M} M_d$$

10. Polymer:

$$P_c \xleftrightarrow{\varphi_P} P_d$$

11. Primary radicals:

$$R^{\bullet}_{in,c} \xleftrightarrow{\varphi_{R^{\bullet}_{in}}} R^{\bullet}_{in,d}$$

12. Macroradicals:

$$R^{\bullet}_c \xleftrightarrow{\varphi_{R^{\bullet}}} R^{\bullet}_d$$

where φ is a partition coefficient between the continuous and dispersed phases. The subscript "d" designates a continuous phase species.

To maintain generality we are permitting all reaction species to partition between the continuous and dispersed phases. The mass transfer is assumed to be rapid, as is the norm in heterophase polymerizations of water-soluble monomers [8].

13. Precipitation because of solubility:

$$R^{\bullet}_{c,kcr-1} + M_c \xrightarrow{k_p} R^{\bullet}_{c,kcr} \xrightarrow{k_D} R^{\bullet}_{d,kcr} \xrightarrow{k_t^*} \text{Inert Product}$$

Where $k_p \gg k_D$ and $k_p \gg k_t$. The subscripts "c", "d", "kcr" designate continuous phase, dispersed phase and critical chain length for macroradical solubility, respectively.

3.1.3. Reactions in the disperse phase (polymer, solvent, monomer and initiator)

14. Initiator decomposition:

$$I_d \xrightarrow{k_{dd}} 2R^{\bullet}_{in,d} \quad (8)$$

I and $R^{\bullet}_{in}$ are the symbols for initiator and primary radicals.

15. Monomer-enhanced decomposition of the initiator

[5]:

$$I_d + M_d \xrightarrow{k'_{dd}} R^{\bullet}_{1,d} + R^{\bullet}_{in,d} \quad (9)$$

16. Initiation:

$$R^{\bullet}_{in,d} + M_d \xrightarrow{k_{p1d}} R^{\bullet}_{1,d} \quad (10)$$

17. Propagation:

$$R^{\bullet}_{r,d} + M_d \xrightarrow{k_{pd}} R^{\bullet}_{r+1,d} \quad (11)$$

18. Transfer [5,7]:

$$R^{\bullet}_{r,d} + M_d \xrightarrow{k_{fmd}} M^{\bullet}_d + P_r \quad (12)$$

$$R^{\bullet}_{r,d} + S_d \xrightarrow{k_{fsd}} S^{\bullet}_d + P_r \quad (13)$$

19. Termination [7]:

$$R^{\bullet}_{r,d} + R^{\bullet}_{s,d} \xrightarrow{k_{tdd}} P_r + P_s \quad (14)$$

To maintain generality, the complete set of initiation, propagation, transfer and termination steps are included in both the continuous and dispersed phases. These will be developed into a general kinetic model, which will be simplified based on experimental observations.

3.2. Definition of the kinetic model parameters

The following parameters will be utilized in the kinetic modeling and are defined to facilitate the subsequent derivation.

3.2.1. Species molar and volume fraction coefficients, ϕ

The "ϕ" parameters summarized below are molar ratios of species in the continuous phase relative to total number of moles or volume in both the continuous and dispersed phases:

$$\phi_{R^{\bullet}_{in}} = \frac{N_{R^{\bullet}_{in,c}}}{N_{R^{\bullet}_{in}}} = \frac{N_{R^{\bullet}_{in,c}}}{N_{R^{\bullet}_{in,c}} + N_{R^{\bullet}_{in,d}}}, \quad (15)$$

$$\phi_{R^{\bullet}} = \frac{N_{R^{\bullet}_c}}{N_{R^{\bullet}}} = \frac{N_{R^{\bullet}_c}}{N_{R^{\bullet}_c} + N_{R^{\bullet}_d}}, \quad (16)$$

$$\phi_M = \frac{N_{M_c}}{N_M} = \frac{N_{M_c}}{N_{M_c} + N_{M_d}}, \quad (17)$$

$$\phi_P = \frac{N_{P_c}}{N_P} = \frac{N_{P_c}}{N_{P_c} + N_{P_d}}, \quad (18)$$

$$\phi_I = \frac{N_{I_c}}{N_I} = \frac{N_{I_c}}{N_{I_c} + N_{I_d}}, \quad (19)$$

$$\phi_V = \frac{V_c}{V_T} = \frac{V_c}{V_c + V_d}, \quad (20)$$

Where $N_{R^{\bullet}_{in}}$, $N_{R^{\bullet}}$, N_I, N_P *and* N_M are symbols representing the moles of primary radicals, macroradicals, initiator, polymer and monomer. V_c and V_d are the volumes of the continuous and dispersed phase respectively. V_T is the total volume of the system ($V_c + V_d$).

3.2.2. Partition coefficients, φ

The partition coefficients (φ) for primary and macro radicals, polymer chains, monomer and initiator are summarized below. The square brackets designate a molar concentration per liter of volume.

$$\varphi_{R^{\bullet}_{in}} = \frac{[R^{\bullet}_{in}]_c}{[R^{\bullet}_{in}]_d}, \quad (21)$$

$$\varphi_{R^{\bullet}} = \frac{[R^{\bullet}]_c}{[R^{\bullet}]_d}, \quad (22)$$

$$\varphi_P = \frac{[P]_c}{[P]_d}, \quad (23)$$

$$\varphi_M = \frac{[M]_c}{[M]_d}, \quad (24)$$

$$\varphi_I = \frac{[I]_c}{[I]_d}. \quad (25)$$

From Eqs. (15)–(25) the molar and volume ratios can be derived for each species. Eq. (26) is the generalized form of the molar ratio.

$$\phi_i = \frac{\varphi_i V_c}{\varphi_i V_c + V_d}, \quad (26)$$

where i corresponds $R^{\bullet}_{in}$, $R^{\bullet}$, M, P and I.

$$V_c = \phi_v V_T \quad (27)$$

$$[R^{\bullet}_{in}]_c = \frac{\phi_{R^{\bullet}_{in}} N_{R^{\bullet}_{in}}}{V_c}, \quad (28)$$

$$[R^{\bullet}]_c = \frac{\phi_{R^{\bullet}} N_{R^{\bullet}}}{V_c}, \quad (29)$$

$$[M]_c = \frac{\phi_M N_M}{V_c}, \quad (30)$$

$$[P]_c = \frac{\phi_P N_P}{V_c}, \quad (31)$$

$$[I]_c = \frac{\phi_I N_I}{V_c}. \quad (32)$$

From Eqs. (21)–(32) the following relations are obtained in

terms of volume fractions

$$[R^{\bullet}_{in}]_c = \frac{\varphi_{R^{\bullet}_{in}}[R^{\bullet}_{in}]}{\varphi_{R^{\bullet}_{in}}\phi_v + (1-\phi_v)}, \quad (33)$$

$$[R^{\bullet}_{in}]_d = \frac{[R^{\bullet}_{in}]}{\varphi_{R^{\bullet}_{in}}\phi_v + (1-\phi_v)}, \quad (34)$$

$$[R^{\bullet}]_c = \frac{\varphi_{R^{\bullet}}[R^{\bullet}]}{\varphi_{R^{\bullet}}\phi_v + (1-\phi_v)}, \quad (35)$$

$$[R^{\bullet}]_d = \frac{[R^{\bullet}]}{\varphi_{R^{\bullet}}\phi_v + (1-\phi_v)}, \quad (36)$$

$$[M]_c = \frac{\varphi_M[M]}{\varphi_M\phi_v + (1-\phi_v)}, \quad (37)$$

$$[M]_d = \frac{[M]}{\varphi_M\phi_v + (1-\phi_v)}, \quad (38)$$

$$[P]_c = \frac{\varphi_P[P]}{\varphi_P\phi_v + (1-\phi_v)}, \quad (39)$$

$$[P]_d = \frac{[P]}{\varphi_P\phi_v + (1-\phi_v)}, \quad (40)$$

$$[I]_c = \frac{\varphi_I[I]}{\varphi_I\phi_v + (1-\phi_v)}, \quad (41)$$

$$[I]_d = \frac{[I]}{\varphi_I\phi_v + (1-\phi_v)}. \quad (42)$$

3.3. Kinetic model development

3.3.1. Balance on initiator molecules

From Eqs.(1)–(14), (37), (38), (41) and (42), the rate of disappearance of initiator can be calculated as

$$\frac{dN_I}{dt} = -k_d[I] - k'_d\alpha[I][M], \quad (43)$$

where

$$\alpha = \frac{\phi_v\varphi_I\varphi_M + (1-\phi_v)}{[\phi_v\varphi_I + (1-\phi_v)][\phi_v\varphi_M + (1-\phi_v)]}, \quad (44)$$

Here α is a grouped parameter including the initiator and monomer partition coefficients and the volume fraction. α would reduce to 1.0 in a homogeneous system.

3.3.2. Balance on primary radicals

From Eqs. (1)–(14), (33), (34), (37), (38), (41) and (42), the rate of disappearance of primary radicals is given by

$$\frac{d[R^{\bullet}_{in}]}{dt} = 2k_d[I] + k'_d\alpha[I][M] - k_{p1}\beta[M][R^{\bullet}_{in}], \quad (45)$$

where α is defined by Eq. (44) and β by

$$\beta = \frac{\phi_v\varphi_{R^{\bullet}_{in}}\varphi_M + (1-\phi_v)}{[\phi_v\varphi_{R^{\bullet}_{in}} + (1-\phi_v)][\phi_v\varphi_M + (1-\phi_v)]}. \quad (46)$$

In a homogeneous polymerization "β" reverts to unity. Applying the Stationary State Hypothesis, $d[R^{\bullet}_{in}]/dt = 0$, to Eq. (45), the total concentration of primary radicals is:

$$[R^{\bullet}_{in}]_{ss} = \frac{2k_d[I] + \alpha k'_d[I][M]}{\beta k_{p1}[M]}. \quad (47)$$

3.3.3. Rate of initiation

The rate of initiation can be expressed as

$$R_I = k'_d\alpha[I][M] + k_{p1}\beta[M][R^{\bullet}_{in}]_{ss}. \quad (48)$$

From Eqs. (47) and (48), one obtains

$$R_I = 2k'_d\alpha[I][M] + 2k_d[I]. \quad (49)$$

To account for the fact that every molecule of initiator which decomposes by thermal bond scission does not generate two polymer molecules, an initiator efficiency factor, f, is introduced

$$R_I = 2[I]\{fk_d + k'_d\alpha[M]\}. \quad (50)$$

From our experimental work, which was discussed in Ref. [1], the order of the initial rate of polymerization was found to be 1.7 with respect to monomer concentration. One would therefore expect that the rate constant for the reaction of initiator with monomer, k'_d , be much greater than the thermal decomposition constant of initiator itself, k_d. The rate of monomer-enhanced ($2\alpha k'_d[M][I]$) is at least 15 times as large as the rate of thermal decomposition ($2fk_d[I]$). This is similar to the situation observed for acrylamide polymerization [9]. Under these circumstances, the expression for rate of initiation simplifies to

$$R_I = 2k'_d\alpha[I][M]. \quad (51)$$

3.3.4. Rate of polymerization

By applying the long chain hypothesis, the rate of polymerization can be assumed to be equal to the rate of monomer disappearance during propagation, and the following equation for the rate of polymerization (R_p) can be derived:

$$R_p = k_{pc}[R^{\bullet}]_c[M]_c\phi_v + k_{pd}[R^{\bullet}]_d[M]_dV_d(1-\phi_v). \quad (52)$$

Substituting the definitions of $[R\bullet]_c$, $[R\bullet]_d$, $[M]_c$, and $[M]_d$ from Eqs. (35)–(38) into Eq. (57) and rearranging, the rate of polymerization can be reduced to its common form

$$R_p = k_{pp}[M][R^{\bullet}], \quad (53)$$

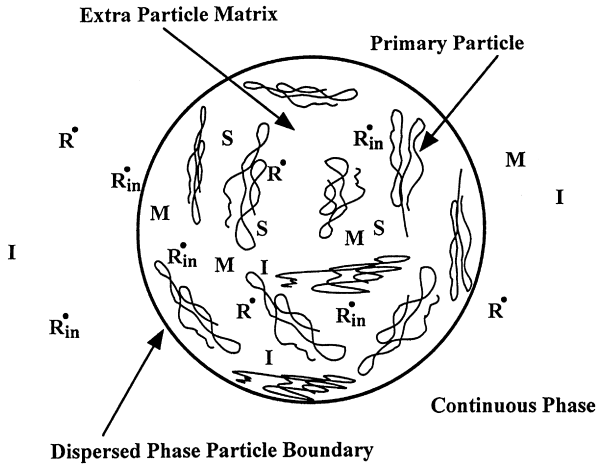

Fig. 1. A schematic of the extra particulate matrix: I = Initiator Molecules, M = Monomer Molecules, S = Solvent Molecules, $R^{\bullet}_{in}$ = Primary Radicals, and $R^{\bullet}$ = Macroradicals.

where k_{pp} is pseudo-propagation constant, which is given by

$$k_{pp} = \frac{k_{pc}\phi_v\varphi_{R\bullet}\varphi_M + k_{pd}(1-\phi_v)}{[\phi_v\varphi_{R\bullet} + (1-\phi_v)][\phi_v\varphi_M + (1-\phi_v)]}, \quad (54)$$

where k_{pp} reduces to k_p for a homogeneous polymerization.

Acrylic acid is completely soluble in toluene, while poly(acrylic acid) is insoluble. Hence the monomer does not penetrate into the poly(acrylic acid) coils which implies that any dispersed phase propagation actually take place in the extra particulate matrix as shown in Fig. 1. This region contains all the species (solvent, initiator, monomer, primary radicals and macroradicals) which are present in the continuous phase. Therefore, provided that the dispersed phase propagation takes place in the extra particle zone between primary particles, it is reasonable to assume that polymerization occurs with the same rate constant as in the continuous phase, i.e. $k_{pc} = k_{pd} = k_p$. From Eq. (54) we therefore have

$$k_{pp} = k_p\gamma, \quad (55)$$

where

$$\gamma = \frac{\phi_v\varphi_{R\bullet}\varphi_M + (1-\phi_v)}{[\phi_v\varphi_{R\bullet} + (1-\phi_v)][\phi_v\varphi_M + (1-\phi_v)]}. \quad (56)$$

γ will have value close to unity and will depend on the dispersed–continuous phase ratio (which is a function of conversion) and the partition coefficients. Fig. 2 shows a plot of γ as a function of conversion for typical values of $\varphi_{R\bullet}$ and φ_M. From Eqs. (53) and (55), it follows that

$$R_p = k_p\gamma[M][R^{\bullet}]. \quad (57)$$

3.3.5. Rate of termination

The total rate of termination by either the disproportion combination or precipitation (solubility) mechanisms is given by

$$R_t = k_{tdc}[R^{\bullet}]_c^2\phi_v + k_{tdd}[R^{\bullet}]_d^2(1-\phi_v) + k_p[M][R^{\bullet}_{kcr-1}]_c\phi_v. \quad (58)$$

Case I. If the termination by disproportion dominates over termination by precipitation mechanism ($k_{td} \gg k_p$), then from Eqs. (35) and (36), the rate of termination then reduces to

$$R_t = k_{tp}[R^{\bullet}]^2, \quad (59)$$

where k_{tp} is the pseudo-termination constant which is given

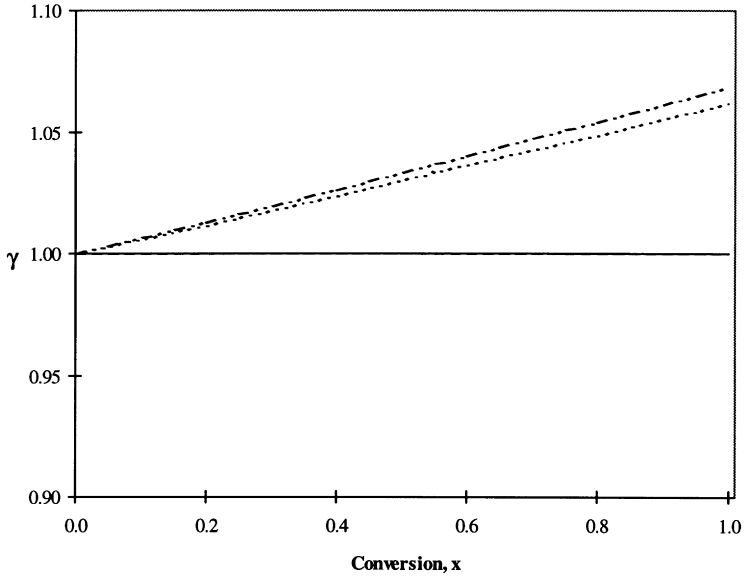

Fig. 2. A plot of γ versus conversion at various value of $\varphi_{R\bullet}$ and φ_M. (— $\varphi_M = 1$, $\varphi_R = 0.01$; – – $\varphi_M = 1$, $\varphi_R = 1$; – – $\varphi_M = 100$, $\varphi_R = 10$ and — – – – $\varphi_M = 100$, $\varphi_R = 100$).

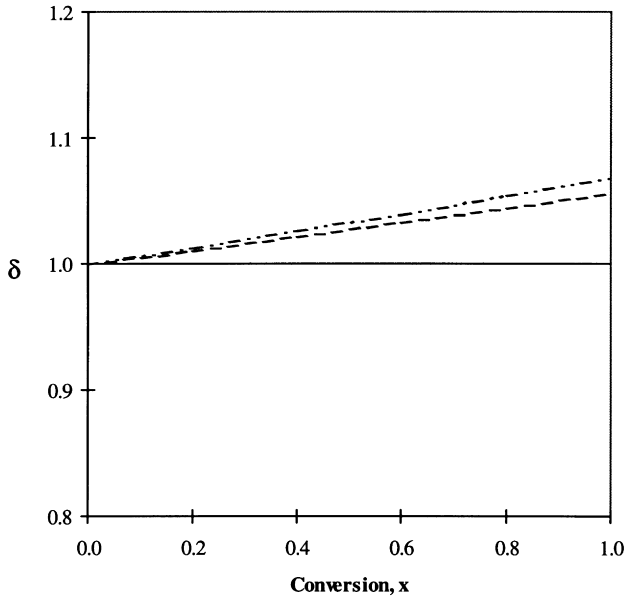

Fig. 3. A plot of δ versus conversion at various value of $\varphi_{R\bullet}$. (— $\varphi_R = 1$, – – $\varphi_R = 10$ and ————$\varphi_R = 100$.)

by

$$k_{tp} = \frac{k_{tdc}\phi_v\varphi_{R\bullet}^2 + k_{tdd}(1-\phi_v)}{[\phi_v\varphi_{R\bullet} + (1-\phi_v)]^2}, \tag{60}$$

where k_{tp} reverts to k_{td} in a homogeneous polymerization.

If one assumes that the marcroradicals terminate prior to full precipitation either in the continuous phase or the extra particle matrix of the dispersed phase, it is reasonable to expect that the termination to occur in both continuous and disperse phase with the same termination constant ($k_{tdc} = k_{tdd} = k_t$). From Eq. (60) the pseudo-termination constant for this case can be calculated as

$$k_{tp} = k_t\delta, \tag{61}$$

where

$$\delta = \frac{\phi_v\varphi_{R\bullet}^2 + (1-\phi_v)}{[\phi_v\varphi_{R\bullet} + (1-\phi_v)]^2}. \tag{62}$$

Therefore, δ is merely a function of the radical partitioning and the conversion, through the volume fraction, ϕ_v with a value close to unity. This is shown in Fig. 3. Further, from Eqs. (59) and (61)

$$R_t = k_t\delta[R^\bullet]^2. \tag{63}$$

At steady state, the rate of initiation equals to the rate of termination. From Eqs. (59) and (61), one obtains

$$2k_d'\alpha[I][M] = k_t\delta[R^\bullet]^2$$

or

$$[R^\bullet] = \frac{\{2k_d'\alpha[I][M]\}^{0.5}}{\{k_t\delta\}^{0.5}}. \tag{64}$$

Substituting $[R^\bullet]$ from Eq. (64) into Eq. (57), the rate of precipitation polymerization is then given by

$$R_p = \frac{k_p\gamma}{k_t^{0.5}}\frac{\{2k_d'\alpha[I]\}^{0.5}[M]^{1.5}}{\delta^{0.5}}. \tag{65}$$

From Eq. (65), the rate order is predicted to be dependent on the monomer concentration to the 1.5 power, in agreement with experimental result as detailed in Ref. [1]. The square-root initiator dependence is also observed.

Case II. If termination by both precipitation and disproportionation are important, one can derive the rate of polymerization expression as follows.

Balance on macroradicals:

$$\frac{d[R^\bullet]}{dt} = R_I - k_t\delta[R^\bullet][R^\bullet] - k_t\delta\,[R^\bullet][R_{in}^\bullet] - k_t[R_{kcr}^\bullet][M],$$

$$\frac{d[R^\bullet]}{dt} = R_I - k_t\delta[R^\bullet]\{[R^\bullet] - [R_{in}^\bullet]\}R_IP^{kcr}. \tag{66}$$

The probability of a macroradical adding a monomer is given by

$$p = \frac{\text{Rate of propogation}}{\sum\text{Rate of competing reactions (non-polymer forming)}}$$

$$= \frac{k_p[M][R^\bullet]}{[R^\bullet]k_t\delta[R_{in}^\bullet] + k_{fm}[M]}.$$

The probability of growing a chain of length kcr (critical chain length) is given by

$$p^{kcr} = \left\{\frac{1}{1 + (k_t\delta\,[R^\bullet])/k_p[M] + k_{fm}/k_p}\right\}^{kcr}. \tag{67}$$

Applying the Stationary State Hypothesis to Eq. (66) one obtains

$$0 = R_I(1-p^{kcr}) - k_t\delta[R^\bullet]\{[R^\bullet] + [R_{in}^\bullet]\}.$$

As $[R_{in}^\bullet] \ll [R^\bullet]$, this equation reduces to

$$k_t\delta[R^\bullet]^2 = R_I(1-p^{kcr}).$$

The total concentration of macroradical is then given by

$$[R^\bullet] = \left(\frac{R_I}{k_t\delta}\right)^{0.5}(1-p^{kcr})^{0.5}. \tag{68}$$

The parameter $(1-p^{kcr})$ is the fraction of the macroradicals, which have chain length less than critical chain length (kcr). From Eqs. (51), (57) and (68), the rate of precipitation polymerization is then given by:

$$R_p = \frac{k_p\gamma}{k_t^{0.5}}\frac{\{2k_d'\alpha[I]\}^{0.5}[M]^{1.5}(1-p^{kcr})^{0.5}}{\delta^{0.5}}. \tag{69}$$

If the termination of macroradicals by precipitation is considered in the mechanism, the macroradical concentration and rate of polymerization are reduced from Case I

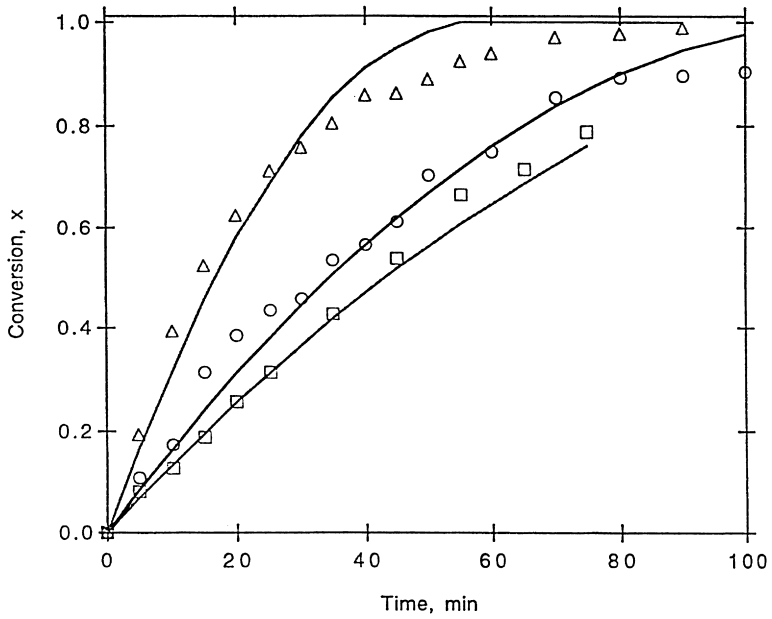

Fig. 4. Simulation results from the kinetic model for the precipitation polymerization of acrylic acid in toluene over a temperature range of 40°C –50°C, $[M]_0 =$ 1.252 mol/l, $[I]_0 = 8.5$ mmol/l and $\varphi_I = \varphi_M = \varphi_{R^\bullet} = 1$. (–□– 40°C, –○– 45°C, –△– 50°C, — model.)

(bimolecular termination by disproportionation exclusively) by a factor $(1 - p^{kcr})^{0.5}$, as is shown in Eqs. (68) and (69). By comparing Eq. (65) with Eq. (69), the modeling with and without termination by precipitation are essentially identical, with the exception of the factor $(1 - p^{kcr})^{0.5}$. If the critical chain length (kcr) is known, this factor can be obtained and used to determine if termination by precipitation plays a significant role in the mechanism. In the precipitation polymerization of acrylic acid in toluene the macroradicals, as well as the polymer molecules were found to precipitate out from the continuous toluene phase at a conversion of approximately 1%. The weight average molecular weight of poly(acrylic acid) at this conversion was found to be 150×10^3 daltons [1]. This corresponds to a chain length of 2081 (normally, critical chain lengths for precipitation are on the molecular level, that is between 5 and 20 monomer units). From experimental results (as discussed in Ref. [1]), transfer to monomer is a chain length controlling step. This implies that k_{fm}/k_p dominates over $k_t \delta[R^\bullet]/k_p[M]$. The value of k_{fm}/k_p is 1.5×10^{-3} for acrylic

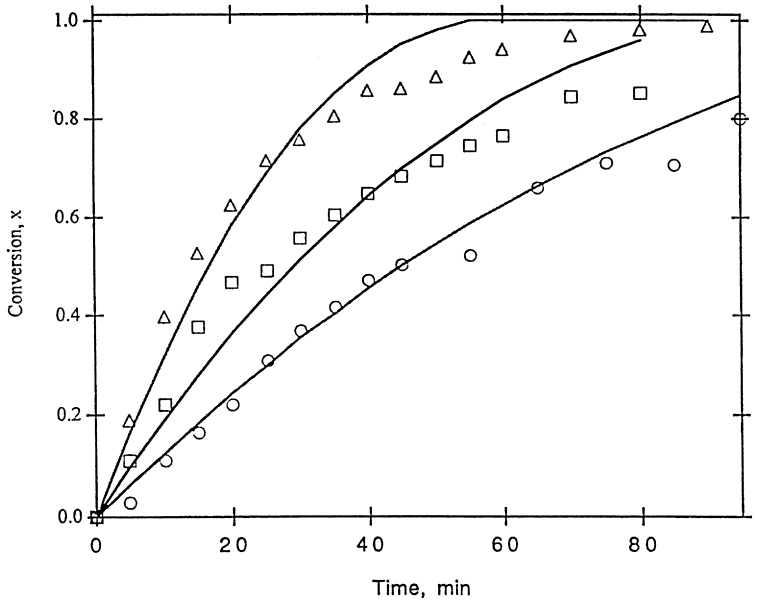

Fig. 5. Simulation results from the kinetic model for the precipitation polymerization of acrylic acid in toluene at 50°C, $[I]_0 = 2$–8.5 mmol/l, $[M]_0 =$ 1.252 mol/l and $\varphi_I = \varphi_M = \varphi_{R^\bullet} = 1$. (–○– $[I]_0 = 2$ mmol/l, –□– $[I]_0 = 6.5$ mmol/l, –△– $[I]_0 = 8.5$ mmol/l, —model.)

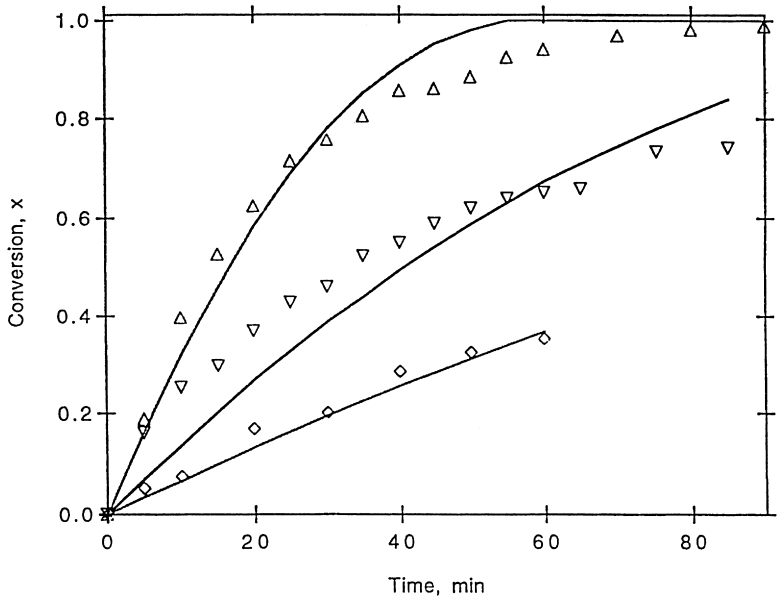

Fig. 6. Simulation results from the kinetic model for the precipitation polymerization of acrylic acid in toluene at 50°C, $[I]_0 = 8.5$ mmol/l, $[M]_0 = 0.156$–1.252 mol/l and $\varphi_I = \varphi_M = \varphi_{R\bullet} = 1$. (–◇– $[M]_0 = 2$ mmol/l, –▽– $[M]_0 = 6.5$ mmol/l, –△– $[M]_0 = 8.5$ mmol/l, — model.)

acid in toluene. Substituting this value and kcr = 2081 into Eq. (67), an estimate of p^{kcr} can be obtained (0.0442). The corresponding value of $(1 - p^{kcr})^{0.5}$ is 0.978. Therefore, from Eq. (69), one can see that the rate of polymerization is reduced by only 2.2% because of the effect of macroradical consumption by precipitation. For this reason, we will consider only the termination by disproportionation and neglect the effect of precipitation on the radical concentration in the model simulation.

3.3.6. Predicting the molecular weight and molecular weight distribution from the kinetic model

The main advantage of the "pseudo-rate constant" method is that it allows us to use the standard free radical homopolymerization equations to determine the molecular weight and the molecular weight distribution in precipitation polymerization. Since the termination by disproportionation dominates over combination in the polymerization of unneutralized acrylic acid [7], the instantaneous number average, $\overline{M}_{Ni}$, and weight average molecular weight, $\overline{M}_{Wi}$, are given by [10] the following equations:

$$\overline{M}_{Ni} = \frac{M_0}{\tau}, \tag{70}$$

$$\overline{M}_{Wi} = \frac{2M_0}{\tau}, \tag{71}$$

where

$$\tau = \frac{k_{tp}R_p}{k_{pp}^2[M]} + \frac{k_{fm}}{k_{pp}} + \frac{k_{fs}[S]}{k_{pp}[M]} \tag{72}$$

and M_0 is the monomer molecular weight (72.06 for acrylic acid).

3.4. Evaluating the kinetic model against experimental data

3.4.1. Rate of precipitation polymerization

The rate of polymerization is given by Eq. (69). This equation can be re-expressed in terms of conversion as

$$\frac{dx}{dt} = \frac{k_p}{k_t^{0.5}} \frac{\gamma\{[2k_d'\alpha[I]\}^{0.5}[M]^{0.5}(1-x)^{0.5}}{\delta^{0.5}}, \tag{73}$$

where α, γ, and δ are grouped parameters which include partition coefficient and volume fractions and are defined by Eqs. (44), (56) and (62), respectively. Simulations were carried out by numerically solving Eq. (73) simultaneously with Eqs. (44), (56) and (62) under various experimental conditions. Different values of the initiator partition coefficients (φ_I), monomer partition coefficients (φ_M) and mecroradical partition coefficients ($\varphi_{R\bullet}$) were also utilized.

The kinetic model can predict the conversion versus time behavior quite reasonably as shown in Figs. 4–6. The Fig. 4 is a conversion-time plot at temperatures between 40°C and 50°C. One can observe a good fit up to 80% conversion. However at lowest temperature (40°C), a limiting conversion is observed. This may be because of the longer induction time, which has consumed a fraction of initial initiator [1]. Fig. 5 shows a conversion-time plot at various initiator concentrations. The kinetic model again provides good agreement with the kinetic data up to a conversion of 80%. However at highest initiator level, and for conversion

Table 1
The kinetic parameters used in the simulations with literature values for comparison

Parameter	Value	Source
$(k_P k'_d 0.5)/k_t^{0.5}$	2.0×10^{-3} mol l^{-1} s^{-1}	This work
$k_p/k_t^{0.5}$	0.531 (l mol^{-1} s^{-1})$^{0.5}$	[11]
k'_d	2.2×10^{-4} l mol^{-1} s^{-1}	This work
k_d	1.81×10^{-5} s^{-1}	[11]
k_{fm}/k_P	1.5×10^{-3}	This work
k_{fm}/k_P	0.02×10^{-3}	[11]

above 70%, slight deviations are observed. Fig. 6 shows the kinetic data as a function of the monomer concentration. The curves are clearly non-linear (1.7th order dependence [1]) and indicate that the monomer concentration has a significant effect on the kinetics, as was also observed by Hunkeler [9].

The model predictions at intermediate initial monomer concentrations are adequate. Clearly, a close "fit" could be obtained if each kinetic curve was regressed independently. However, one would have less confidence in the parameter estimates. Therefore, the authors have elected to regress all the data at the same time, obtaining a more robust estimation at the expense of the slight deviations for certain data sets.

The kinetic constants and the other parameters regressed in this investigation are compared with the value from literature in Table 1. The rate of monomer-enhanced decomposition obtained from this investigation was approximately 15 times higher than the rate of thermal decomposition constant for initiator. This implies that the monomer-enhanced decomposition step dominates thermal decomposition as in indicated by the experimental data presented in Ref. [1]. A high rate of monomer enhanced decomposition has also been reported for other acrylic water soluble polymers such as acrylamide and cationnic quaternary ammonium [9].

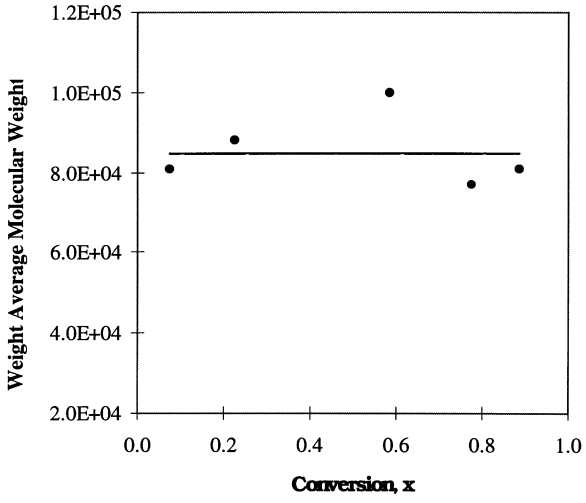

Fig. 7. Experimental (weight average molecular weight data versus conversion) for the precipitation polymerization of acrylic acid in toluene at 50°C, $[M]_0 = 1.252$ mol/l, $[I]_0 = 8.5$ mmol/l and $\varphi_M = 1$.

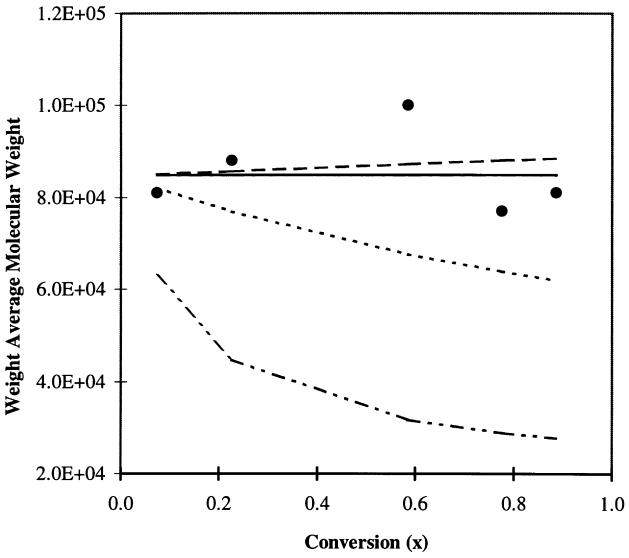

Fig. 8. Simulation results (weight average molecular weight versus conversion) for the precipitation polymerization of acrylic acid in toluene at 50°C, $[M]_0 = 1.252$ mol/l, $[I]_0 = 8.5$ mmol/l and $\varphi_M = 10$. (——— $\varphi_R = 0.01$; -- $\varphi_R = 0.1$, — $\varphi_R = 1$, – – – $\varphi_R = 10$, ——— $\varphi_R = 100$ and ● Experimental data.)

3.4.2. Weight average molecular weight

From experimental results as detailed in Ref. [1], we found that transfer to monomer is the chain controlling

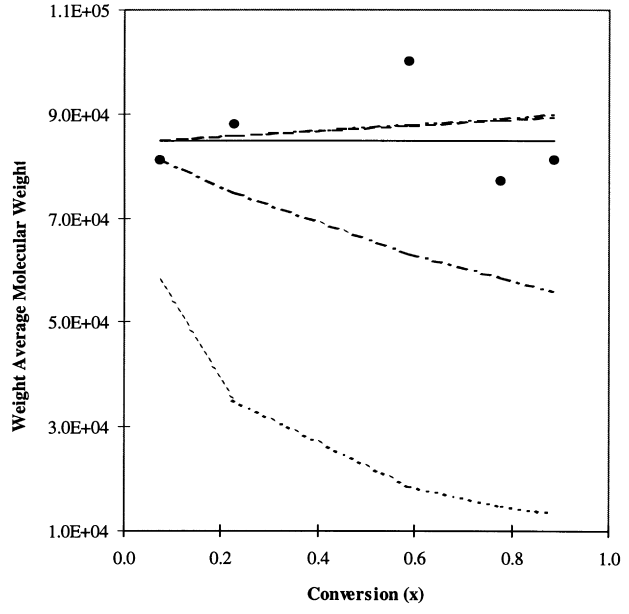

Fig. 9. Simulation results (weight average molecular weight versus conversion) for the precipitation polymerization of acrylic acid in toluene at 50°C, $[M]_0 = 1.252$ mol/l, $[I]_0 = 8.5$ mmol/l and $\varphi_M = 100$. (-- $\varphi_R = 0.01$; ——— $\varphi_R = 0.1$, — $\varphi_R = 1$, – – – $\varphi_R = 10$, – – – $\varphi_R = 100$ and ● Experimental data.)

reaction. Therefore, using Eqs. (71) and (72), the instantaneous weight average molecular weight is given by

$$\overline{M}_{wi} = \frac{2M_0 k_{pp}}{k_{fm}}. \quad (74)$$

The simulations were carried out by numerically solving Eq. (74) simultaneously with Eqs. (55) and (56). Various values for parameters such as the monomer partition coefficients (φ_M) and macroradical partition coefficients ($\varphi_{R\bullet}$) were employed. The kinetic constant regressed from this data are listed in Table 1. The predicted weight average molecular weight as a function of conversion is compared to the experimental data for various parameter values in Figs. 7–9. From these figures, the kinetic model is seen to fit the experimental data well when the monomer partition coefficients (φ_M) and macroradical partition coefficients ($\varphi_{R\bullet}$) are greater or equal to unity. The sensitivity of the molecular weight to the partition coefficient is low for values above unity and we can not find narrow confidence intervals for φ_M or $\varphi_{R\bullet}$ from our regression. This would require a separate experimental investigation in a non-reactive system. This is not, however, necessary since most kinetic models [8], this one included, predict the molecular weight well without precise estimates of the partition coefficients. Based on these simulations, we can bind the initiator, monomer and macroradical partition coefficients as follows;

$$\varphi_I \cong \varphi_M \geq 1.0 \qquad \text{and} \qquad \varphi_{R\bullet} \geq 1.0.$$

As this range do not exclude unity, and there is no reason to expect initiator, monomer or macroradicals to favor the continuous or dispersed phase, an equi-partitioning assumption is reasonable as a first approximation.

4. Conclusions

A mechanistic model was developed, based on an elementary reaction scheme for precipitation polymerization and was found to predict the conversion and the weight-average molecular weight very well. The mechanism consists of the initiation, propagation, transfer and termination reactions, which are common to all free-radical polymerizations. It also found that monomer-enhanced decomposition and transfer to monomer are the dominant mechanisms for initiation and termination reactions respectively. The kinetic model predicts that both monomer partition coefficient and macroradicals partition coefficients are greater or equal to unity. These imply that the polymerization reactions occur in both continuous and dispersed phases, validating the derivation of heterogeneous mechanism. The kinetic model developed herein was based on pilot scale data and can be utilized for reactor design purposes.

References

[1] Bunyakan C, Hunkeler D. Polymer 1999;40:6213.
[2] Avela A, Poersch HG, Reichert KH. Die Angewandte Makromolecular Chemie 1990;175:107.
[3] Poersch HG, Avela A, Reichert KH. Die Angewandte Makromolecular Chemie 1993;206:157.
[4] Kabanov VA, Topchiev DA, Karaputadze TM. J Polym Sci 1973;C42:173.
[5] Manickam SP, Venkataro K, Subbaratnam NR. Eur Polym J 1979;15:483.
[6] Gromov VF, Galaperina NI, Osmanov TO, Khomikovski PM, Abkin AD. Eur Polym J 1980;16:529.
[7] Hruska V. Aqueous polymerization of partially neutralized acrylic acid. MS Thesis. McMaster University, Hamilton, Ont, Canada, 1984.
[8] Hunkeler D, Hamielec AE, Baade W. Polymer 1989;30:127.
[9] Hunkeler D. Macromolecules 1991;24(9):2160.
[10] Rudin A. The elements of polymer science and engineering. New York: Academic Press, 1982.
[11] Brandrup J, Immergut EH. Polymer handbook. New York: Wiley, 1975.